European Control Conference
July 16, 2015

Stabilization and Trajectory Tracking of Version and Vergence Eye Movements in Human Binocular Control

Takafumi Oki[1] and Bijoy K. Ghosh[2]

***Abstract*— Using the well known approach of *feedback linearization*, we study problems that can be applied to controlling the rotational motion of a pair of human eyes. Eyes move to acquire a fixed point target and the control task is to direct the eye-pair towards a general target direction and, if the target is close by, to focus on the target. Roughly speaking, the former task is accomplished by *versional eye movements* and the latter task of pinpointing the eye on a specific target is accomplished by *vergence eye movements*. In this paper, we separately synthesize *asymptotically stabilizing controllers*, in the neighborhood of a target point, for version and vergence control systems. This is accomplished by defining a suitable output and regulating the output to the origin, while the eyes gaze towards the target.**

I. INTRODUCTION

Human eye movement can be looked at, as a rotational dynamics on the space **SO(3)** with constraints that have to do with the axis of rotation. Specifically, it has been observed that the oculomotor system chooses just one angle of ocular torsion for any one gaze direction. This choice is governed by what is now well known as the Listing's Law, which we now explain. Any eye orientation can be reached, starting from one specific orientation, called the primary orientation[1], by rotation about a single axis. Listing's Law states that this axis is restricted to lie on a plane called the Listing's Plane. Typically, the Listing's plane is observed (see for example Tweed and Vilis [1], [2]) to be perpendicular to the primary axis. Consequently, the set of all orientations the eye can assume is a sub-manifold of **SO(3)**. While gazing targets located at optical infinity and keeping the head fixed, eye orientations are restricted to this sub-manifold [3], called **LIST**. For a detailed discussion about the sub-manifold **LIST**, we would refer to [4].

While Listing's law adequately describes monocular eye movements when head is assumed to be fixed, this is not the case when two eyes are involved and when head is assumed to be free [5]. In this paper, we are primarily concerned with head fixed binocular vision, where Listing's law is not valid for fixation of nearby targets. It has been observed by Rijn and Berg [6] (see also Nakayama [7]), that when a pair of human eyes fixate on a nearby point target, the orientations of the two eyes do not satisfy the Listing's law. The eye rotations are not independently controlled, but can be viewed as a concatenation of version followed by vergence. The versional component of the eye movement is identical for both the eyes and satisfies Listing's law. This is equivalent to saying that the versional part of the eye rotation belongs to **LIST**. On the other hand, the vergence component of the eye movement rotates the two eyes in opposite directions, in order to fixate nearby point targets. Following [6], we would assume that for the vergence part, the rotation vector is restricted to the mid-sagittal plane with respect to the fixed head coordinate system [2]. Starting from the primary orientation, the set of all orientations that are achievable using rotations with axes in the mid-sagittal plane is a sub-manifold **MS** of **SO(3)**. We have introduced a Riemannian metric for **LIST** and **MS** and write down the associated Euler Lagrange equations that describe the version and vergence eye dynamics (see [8]). These two eye dynamics were also studied, and introduced for the first time, in [9] wherein we study eye movement as a tracking control problem.

In this paper, we introduce asymptotically stabilizing controllers for the two dynamics. We make the final gaze direction asymptotically stable and the 'trajectory to be tracked' invariant and asymptotically stable as well.

A. Notations

Throughout this paper, let $\mathbb{R}$ denote the set of real numbers. Let $\mathbb{R}^n$ be the set of n dimensional real vectors and let $\mathbb{R}^{n\times n}$ denote the set of $n \times n$ matrices with real numbers. Moreover, let $\mathbb{S}^n$ be the n dimensional unit sphere in $\mathbb{R}^{n+1}$. For a given vector x and matrix A, let x^T and A^T denote their transposes, respectively. For given vectors x and $y \in \mathbb{R}^n$, $\langle x, y\rangle = x^T y$ stands for the standard inner product on $\mathbb{R}^n$. Finally for vectors x and $y \in \mathbb{R}^3$, $x \times y$ denotes a vector cross product on $\mathbb{R}^3$.

II. QUATERNION AND SO(3)

In the discussion of human eye and head movement problems [4], [8], [10], [11], quaternion plays an important role to represent the rotational dynamics on **SO(3)** and on sub-manifolds of **SO(3)**. In this section, we review some basic concepts of the quaternion [12].

Let $q = [\, q_0 \;\; q_1 \;\; q_2 \;\; q_3 \,] \in \mathbb{S}^3 \subset \mathbb{R}^4$. Let $\mathbf{Q}$ be the set of unit quaternion and define an unit quaternion as

$$q = q_0 + q_1\,\mathbf{i} + q_2\,\mathbf{j} + q_3\,\mathbf{k} \in \mathbf{Q} \tag{1}$$

*Partially supported by the National Science Foundation under grant 1029178

[1]Takafumi Oki and Bijoy K. Ghosh are with the Department of Mathematics and Statistics, Texas Tech University, Lubbock, TX, USA. bijoy.ghosh@ttu.edu

[1]The primary orientation is often chosen to coincide with the frontal gaze direction.

[2]The point midway between the center of the two eyes is called the ego-center. The mid-sagittal plane is the plane perpendicular to the segment joining the center of the two eyes and passing through the ego-center.

where $\mathbf{i}$, $\mathbf{j}$, and $\mathbf{k}$ are imaginary units. In (1), q_0 is called the $scalar$ part and $[\, q_1 \;\; q_2 \;\; q_3 \,]^T$ is called the $vector$ part of the quaternion denoted by

$$vec(q) = [\, q_1 \;\; q_2 \;\; q_3 \,]^T. \tag{2}$$

For a given unit vector $v = [\, v_1 \, v_2 \, v_3 \,] \in \mathbb{S}^2$, the unit quaternion acts on v as a rotation operator

$$vec(q \cdot (v_1\mathbf{i} + v_2\mathbf{j} + v_3\mathbf{k}) \cdot q^*) \tag{3}$$

where $*$ is quaternion conjugate and $\cdot$ is quaternion multiplication [12]. The vector in (3) is obtained by rotating the vector v using a rotation matrix in **SO(3)**. Define a map rot between $\mathbf{Q} \to \mathcal{R}(q) \in \mathbf{SO(3)}$ as

$$rot(q) = \begin{bmatrix} q_0^2 + q_1^2 - q_2^2 - q_3^2 & 2\,(q_1q_2 - q_0q_3) & 2\,(q_1q_3 + q_0q_2) \\ 2\,(q_1q_2 + q_0q_3) & q_0^2 + q_2^2 - q_1^2 - q_3^2 & 2\,(q_2q_3 - q_0q_1) \\ 2\,(q_1q_3 - q_0q_2) & 2\,(q_2q_3 + q_0q_1) & q_0^2 + q_3^2 - q_1^2 - q_2^2 \end{bmatrix} \tag{4}$$

The map $rot(q)$ is onto and 2 to 1 because a pair of antipodal unit quaternion maps onto identical elements of $\mathbf{SO(3)}$, i.e $rot(q) = rot(-q)$ and it is equivalent to

$$rot(q)v = vec(q \cdot (v_1\mathbf{i} + v_2\mathbf{j} + v_3\mathbf{k}) \cdot q^*). \tag{5}$$

We characterize the rotation operation $rot(q)v$ by an axis-angle parametrization

$$(\, \theta, \, \phi, \, \alpha \,) \in [\, -\pi \;\; \pi \,] \times [\, 0 \;\; 2\pi \,] \times \left[\, -\tfrac{\pi}{2} \;\; \tfrac{\pi}{2} \,\right]. \tag{6}$$

In the axis-angle parametrization, the axis of rotation vector $\bar{n}$, an eigenvector of the rotation matrix corresponding to the eigenvalue 1, is parameterized as

$$\bar{n} = [\, \cos\theta \cos\alpha \;\; \sin\theta \cos\alpha \;\; \sin\alpha \,]^T \in \mathbb{S}^2 \tag{7}$$

and the quaternion are parameterized as

$$\begin{aligned} q(\theta, \phi, \alpha) &= [\, \cos\tfrac{\phi}{2} \;\; \sin\tfrac{\phi}{2}\, \bar{n}^T \,]^T \\ &= \begin{bmatrix} \cos\frac{\phi}{2} \\ \sin\frac{\phi}{2}\cos\theta\cos\alpha \\ \sin\frac{\phi}{2}\sin\theta\cos\alpha \\ \sin\frac{\phi}{2}\sin\alpha \end{bmatrix} \in \mathbb{S}^3. \end{aligned} \tag{8}$$

We set $v = [\, 0 \;\; 0 \;\; 1 \,]^T \in \mathbb{S}^2$ as the $primary\ gaze\ direction$ and define a map $proj$ from $(\, \theta, \, \phi, \, \alpha \,)$ to $\mathbb{S}^2$ by

$$\begin{aligned} proj(rot(q)) &= rot(q(\theta, \phi, \alpha))v \\ &= \begin{bmatrix} \sin\theta\sin\phi\cos\alpha + \cos\theta\sin^2\frac{\phi}{2}\sin\alpha \\ -\cos\theta\sin\phi\cos\alpha + \sin\theta\sin^2\frac{\phi}{2}\sin\alpha \\ \cos^2\frac{\phi}{2} - \sin^2\frac{\phi}{2}\cos 2\alpha \end{bmatrix}. \end{aligned} \tag{9}$$

Geometric interpretation of the vector in (9) is that v is rotated around the axis $\bar{n}$ by counter clockwise angle ϕ.

III. DYNAMICAL SYSTEM ON **LIST** AND **MS**

A. Version and Vergence Eye Movement

A typical human eye rotation can be described as a dynamical system on **SO(3)** with constraints imposed on the axis of rotation $\bar{n}$ in (7). A typical eye movement can be decomposed into two processes which are called 'version' and 'vergence'. In the version process, both eyes move synchronously and symmetrically in the same direction and the axis of rotation is restricted to the Listing's plane [1], [2]. In the vergence process, the eyes move to opposite direction and the axis of rotation is restricted to the mid-sagittal plane [6]. These constraints on the axis of rotation yields sub-manifolds [13] of **SO(3)** which are called **LIST** and **MS**.

B. Euler-Lagrange Systems on Sub-manifolds of **SO(3)**

In this subsection, we introduce rotational dynamical systems on sub-manifolds **LIST** and **MS** [4], [8] of **SO(3)**, for the purpose of describing version and vergence eye movement control systems. Following [3], [10], [11] we observe that the axis-angle parametrization (θ, ϕ, α) in (6) defines a Riemannian metric on **SO(3)** given by

$$G_{\mathbf{SO(3)}}(\theta, \phi, \alpha) = \mathrm{diag}\left\{ \sin^2\tfrac{\phi}{2}\cos^2\alpha, \;\; \tfrac{1}{4}, \;\; \sin^2\tfrac{\phi}{2} \right\} \in \mathbb{R}^{3\times 3} \tag{10}$$

where the symbol 'diag' denotes a diagonal matrix of appropriate dimension. For the sub-manifold **LIST**, the axis of rotation $\bar{n}$ in (7) is constrained by $\alpha = 0$. It follows that

$$\bar{n}(\theta, 0) = [\, \cos\theta \;\; \sin\theta \;\; 0 \,]^T \in \mathbb{S}^2. \tag{11}$$

For the submanifold **MS**, we set $\theta = \frac{\pi}{2}$ for $\bar{n}$ in (7) and obtain

$$\bar{n}(\tfrac{\pi}{2}, \alpha) = [\, 0 \;\; \cos\alpha \;\; \sin\alpha \,]^T \in \mathbb{S}^2. \tag{12}$$

Riemannian metrics for the two sub-manifolds are given by setting $\alpha = 0$ and $\theta = \frac{\pi}{2}$ in (10), to obtain

$$\begin{aligned} G_{\mathbf{LIST}}(\theta, \phi) &= \mathrm{diag}\left\{ \sin^2\tfrac{\phi}{2}, \;\; \tfrac{1}{4} \right\} \in \mathbb{R}^{2\times 2} \\ G_{\mathbf{MS}}(\alpha, \phi) &= \mathrm{diag}\left\{ \sin^2\tfrac{\phi}{2}, \;\; \tfrac{1}{4} \right\} \in \mathbb{R}^{2\times 2}. \end{aligned} \tag{13}$$

The matrices (13) define Geodesic equations on **LIST** and **MS** sub-manifolds given by the well known Euler-Lagrange (EL) formula

$$\frac{d}{dt}\frac{\partial L}{\partial \dot{\eta}} - \frac{\partial L}{\partial \eta} = \tau, \;\; \text{where } L(\eta, \dot{\eta}) = \dot{\eta}^T G(\eta)\dot{\eta} \tag{14}$$

and where η is either $[\, \theta \;\; \phi \,]^T$ or $[\, \alpha \;\; \phi \,]^T$ and τ is the generalized torque, to be viewed as the external input. Riemannian metrics for the two sub-manifolds, in (13), have identical structure, leading to dynamical systems that have inherent similarities. However, the domain of the two systems and the range of the map $proj$ in (9) are different.

Following Rajamuni et. al. [8], we now define a dynamical system on **LIST** and **MS**. Let $x = [x_1, x_2, x_3, x_4]^T$ be state variables where $x_2 = \dot{x}_1$ and $x_4 = \dot{x}_3 \in \mathbb{R}$. For **LIST**, the states x_1 and x_3 are the angle variables θ and ϕ, respectively. Likewise for **MS**, the states x_1 and x_3 are the angle variables α and ϕ, respectively. Define domains

$$\begin{aligned} \mathcal{X}_{\mathbf{LIST}} &= \{(x_1, x_3) \mid \;\; x_1 \in [-\pi \;\; \pi\,], \, x_3 \in (0 \;\; 2\pi) - \{\pi\}\} \text{ and} \\ \mathcal{X}_{\mathbf{MS}} &= \{(x_1, x_3) \mid \;\; x_1 \in \left(-\tfrac{\pi}{2} \;\; \tfrac{\pi}{2}\right), \, x_3 \in (0 \;\; 2\pi)\}. \end{aligned} \tag{15}$$

On the state space $\mathcal{X}_{\textbf{LIST}} \times \mathbb{R}^2$ and $\mathcal{X}_{\textbf{MS}} \times \mathbb{R}^2$, the EL formula (14) provides description of a dynamical system given by

$$\begin{aligned}\dot{x} &= f(x) + g_1(x)u_1 + g_2(x)u_2 \\ &= \begin{bmatrix} x_2 \\ -x_2\, x_4 \cot\frac{x_3}{2} \\ x_4 \\ x_2^2 \sin x_3 \end{bmatrix} + \begin{bmatrix} 0 \\ \csc^2\frac{x_3}{2} \\ 0 \\ 0 \end{bmatrix} u_1 + \begin{bmatrix} 0 \\ 0 \\ 0 \\ 4 \end{bmatrix} u_2 \end{aligned} \tag{16}$$

where u_1 and u_2 are the external control inputs. Using the definition of $proj$ in (9), we define system outputs that are called $version$ and $vergence$ output maps, described by

$$y_{vs}(x_1, x_3) = \begin{bmatrix} \sin x_1 \sin x_3 \\ -\cos x_1 \sin x_3 \\ \cos x_3 \end{bmatrix}, \tag{17}$$

and

$$y_{vg}(x_1, x_3) = \begin{bmatrix} \sin x_3 \cos x_1 \\ \sin^2\frac{x_3}{2} \sin 2x_1 \\ \cos^2\frac{x_3}{2} - \sin^2\frac{x_3}{2} \cos 2x_1 \end{bmatrix}. \tag{18}$$

Note that the dynamical system (16) has a singularity at $x_3 = 0$ or 2π resulting from the Riemannian metric (13).

For the version and vergence problems, we consider the dynamical system (16) with output mappings y_{vs} and y_{vg}, respectively. We obtain partial derivatives of the version and vergence output mappings described as follows:

$$\frac{\partial y_{vs}}{\partial x_1} = \begin{bmatrix} \cos x_1 \sin x_3 \\ \sin x_1 \sin x_3 \\ 0 \end{bmatrix}, \quad \frac{\partial y_{vs}}{\partial x_3} = \begin{bmatrix} \sin x_1 \cos x_3 \\ -\cos x_1 \cos x_3 \\ -\sin x_3 \end{bmatrix} \tag{19}$$

and

$$\frac{\partial y_{vg}}{\partial x_1} = \begin{bmatrix} -\sin x_3 \sin x_1 \\ 2\sin^2\frac{x_3}{2} \cos 2x_1 \\ 2\sin^2\frac{x_3}{2} \sin 2x_1 \end{bmatrix}, \quad \frac{\partial y_{vg}}{\partial x_3} = \begin{bmatrix} \cos x_3 \cos x_1 \\ \frac{1}{2}\sin x_3 \sin 2x_1 \\ -\sin x_3 \cos^2 x_1 \end{bmatrix} \tag{20}$$

We now state and prove the following:

Proposition 3.1: On $\mathcal{X}_{\textbf{LIST}}$ and $\mathcal{X}_{\textbf{MS}}$, the output mapping y_{vs} and y_{vg} are non-degenerate. Boundaries of the two domains are mapped to $(0, 0, \pm 1)$ and $(0, 0, 1) \in \mathbb{S}^2$, respectively.

Proof: By substituting specific values into partial derivatives, we see that a pair of partial derivatives $\{\frac{\partial y_{vs}}{\partial x_1}, \frac{\partial y_{vs}}{\partial x_3}\}$ is degenerate (i.e $\dim\{\frac{\partial y_{vs}}{\partial x_1}, \frac{\partial y_{vs}}{\partial x_3}\} < 2$) at $x_3 = 0, \pi$, and 2π. A pair $\{\frac{\partial y_{vg}}{\partial x_1}, \frac{\partial y_{vg}}{\partial x_3}\}$ is degenerate at $x_1 = \pm\frac{\pi}{2}$ or $x_3 = 0$ and 2π. ■

In Fig. 1, the output functions y_{vs} and y_{vg} are sketched as a function of the angle variables, for the sub-manifolds **LIST** and **MS** respectively. Fig. 1a is for **LIST** where the axis of rotation $\bar{n}$ (11), is restricted to the YZ plane. The figure shows three axes of rotations indicated by three arrows, for three different values of θ ($\theta = 0, \frac{3\pi}{4}, \frac{2\pi}{3}$). For a specific θ corresponding to an axis of rotation, the output function y_{vs} is plotted as a function of ϕ. These plots are shown as great circles starting from the point $(0, 0, 1)$. All trajectories of y_{vs} with a distinct value of θ intersect at points $(0, 0, \pm 1)$ which corresponds to $\phi = 0$ and π respectively.

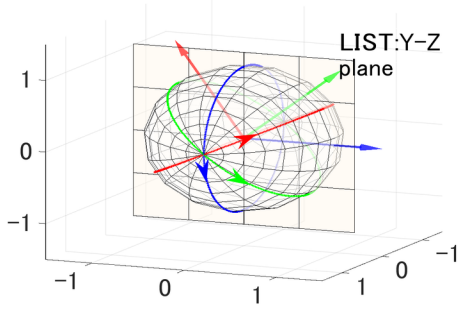

(a) Version Output

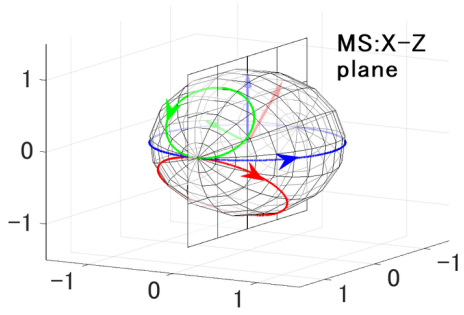

(b) Vergence Output

Fig. 1: Version and Vergence output functions are plotted: In (a), the blue, green, and red lines are trajectories of y_{vs} with $\theta = 0, \frac{3\pi}{4}$ and $\frac{2\pi}{3}$. In (b), the blue, green, and red lines are y_{vg} with $\alpha = 0, \frac{\pi}{3}$ and $-\frac{\pi}{4}$.

Fig. 1b is for **MS** where the axis of rotation $\bar{n}$ (12), is restricted to the XZ plane. The figure shows three axes of rotations indicated by three arrows, for three different values of α ($\alpha = 0, \frac{\pi}{3}, -\frac{\pi}{4}$). For a specific α corresponding to an axis of rotation, the output function y_{vg} is plotted as a function of ϕ. These plots are shown as circles starting from the point $(0, 0, 1)$. All trajectories of y_{vg} with a distinct value of α intersect at the point $(0, 0, 1)$ which corresponds to $\phi = 0$ or 2π.

IV. VERSION AND VERGENCE EYE CONTROL

We begin this section by describing the main problem considered in this paper. The problem is formulated for version and vergence separately. Because the description of the dynamical system (16) on **LIST** and **MS** are identical, we would drop the subscripts for the version and vergence symbols from output mappings, i.e. the symbol y would be used for both y_{vs} and y_{vg} in (17) and (18) respectively.

Let us denote by y_0 the initial target direction and by y^* the final target direction, the eye is required to attain at the end of a final time $T > 0$. We assume that y^* is chosen in such a way that the plane spanned by y_0 and y^* does not contain the points $(0, 0, \pm 1)$ on $\mathbb{S}^2$. For a unit vector v in $\mathbb{R}^3$, we now define a subset of $\mathbb{S}^2$ as follows:

$$\rho_v := \left\{ y \in \mathbb{S}^2 \,|\, \langle v, y \rangle = 0 \text{ for } v \in \mathbb{R}^3 \right\}. \tag{21}$$

Clearly, if v is chosen perpendicular to the vectors y_0 and y^*, ρ_v is a curve on $\mathbb{S}^2$ joining the two points y_0 and y^*.

The problem we consider in this paper is to design, if possible, a control signal $u(t)$ for $0 \leq t \leq T$ such that

- y^* is a locally asymptotically stable equilibrium point of the system.
- If $y(0) \in \rho_v$ then $y(t) \in \rho_v$ for all $0 \leq t \leq T$ and $y(T) = y^*$ for some $t = T$.
- The set ρ_v is locally asymptotically stable and invariant under the control input u.

In [8], [10], [11], [14], the eye movement control problem is posed as an optimal control problem where the implementation of the control is in the open loop. In [10], [11], the eye movement control problem is also posed as a potential control problem, where the implementation is in the closed loop. In each one of these problems, the goal is to transfer the state from an a priori chosen initial point to a final point. The path connecting the two states are not specified a priori. This paper extends earlier work on the eye movement control by forcing the eye to follow a preselected path, viz. described by ρ_v.

A. Control Strategy for A Single Eye

We consider control of eye-gaze direction for a single eye. Our control law can be easily extended to a pair of eyes. We describe this extension, via simulation, in subsection V[3]. We suppose that for both version and vergence control, the eye moves from an initial direction at rest. The control is synthesized using input-state linearization as described in [15].

As described earlier, we would use the symbol y to represent both y_{vs} and y_{vg}. It would follow that $y = y(x)$ is the target direction of the eye corresponding to the state x as described in (17), (18).

Let $\{X, Y, Z\}$ be the head fixed reference frame. We propose to define a new frame $\{n_1, n_2, n_3\}$ (see Fig. 2). We begin by setting $n_3 = y^* \in \mathbb{S}^2 - (0, 0, \pm 1)$. We choose $n_1 = y_0 \times n_3$ and $n_2 = n_1 \times n_3$. The path ρ_{n_1} described in (21) contains the initial direction y_0 and the final target direction y^*. The real number $\langle n_2, y \rangle$ provides a coordinate of the point y on the path ρ_{n_1}. Using the frame $\{n_1, n_2, n_3\}$, we define a new output mapping given by

$$h(x_1, x_3) = \begin{bmatrix} h_1 \\ h_2 \end{bmatrix} = \begin{bmatrix} \langle n_1, y \rangle \\ \langle n_2, y \rangle \end{bmatrix}. \tag{22}$$

The two components of h are projections of y onto the new coordinate vectors n_1 and n_2. Since $\{n_1, n_2, n_3\}$ are orthonormal, it follows that

$$h_3^2 = \langle n_3, y \rangle^2 = 1 - h_1^2 - h_2^2 \tag{23}$$

and

$$\langle n_3, y(t) \rangle \to \pm 1 \text{ if } h_1(t) \text{ and } h_2(t) \to 0 \text{ as } t \to \infty. \tag{24}$$

[3]Initially the two eyes move along identical trajectory, following 'version control system'. Subsequently, the eyes move in opposite directions following 'vergence control system'. Versional control to the two eyes are the same. Vergence control to the eyes are not identical.

Note that when $h_1 = 0$, the vector y is on the path ρ_{n_1}. Additionally when $h_2 = 0$, the vector y is along the target direction y^*.

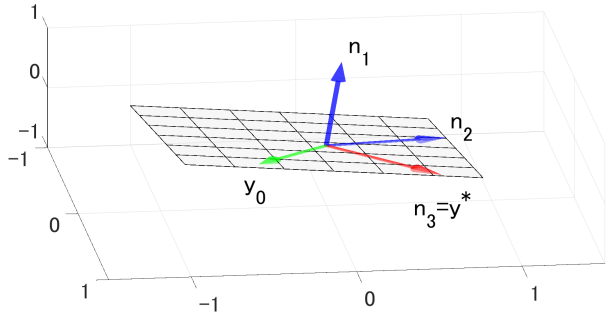

Fig. 2: The unit vector n_1 is normal to the shaded plane spanned by y_0 and y^*.

B. Input-State Linearization

For the dynamical system (16), (22), we proceed to perform input-state linearization as described in [15]. We would freely use the notation $y_{x_j} = \frac{\partial y}{\partial x_j}$, the Lie derivative operator L, and proceed to compute Lie derivatives of the output h along with vector fields $\{f, g_1, g_2\}$.

First order Lie-derivatives of the output h along the vector fields $\{g_1, g_2\}$ are given by

$$L_{g_i} h_j(x) = 0 \text{ for } i, j = 1, 2 \text{ and for any } x_1 \text{ and } x_3 \tag{25}$$

because $y_{x_2} = y_{x_4} = 0$. Next we have

$$\begin{aligned} L_f h_1(x) &= x_2 \langle n_1, y_{x_1} \rangle + x_4 \langle n_1, y_{x_3} \rangle \\ L_f h_2(x) &= x_2 \langle n_2, y_{x_1} \rangle + x_4 \langle n_2, y_{x_3} \rangle \end{aligned} \tag{26}$$

and it would follow that

$$\begin{aligned} L_{g_1} L_f h_1(x) &= \csc^2 \tfrac{x_3}{2} \langle n_1, y_{x_1} \rangle \\ L_{g_2} L_f h_1(x) &= 4 \langle n_1, y_{x_3} \rangle \\ L_{g_1} L_f h_2(x) &= \csc^2 \tfrac{x_3}{2} \langle n_2, y_{x_1} \rangle \\ L_{g_2} L_f h_2(x) &= 4 \langle n_3, y_{x_2} \rangle. \end{aligned} \tag{27}$$

From above equations, we construct a *decoupling matrix* (See [15], page 220) as follows

$$A(x) = \begin{bmatrix} L_{g_1} L_f h_1 & L_{g_2} L_f h_1 \\ L_{g_1} L_f h_2 & L_{g_2} L_f h_2 \end{bmatrix}. \tag{28}$$

If the decoupling matrix $A(x)$ is non-singular on some open neighborhood of a point x°, the system has a relative degree 4. In this case, a local coordinate transformation

$$\xi = \Phi(x) = \begin{bmatrix} h_1(x) \\ L_f h_1(x) \\ h_2(x) \\ L_f h_2(x) \end{bmatrix} \tag{29}$$

exists and it is locally a diffeomorphism. Then the dynamical system (16) has the following form in the new coordinates given by

$$\begin{aligned}
&\dot{\xi_1} = \xi_2 \\
&\dot{\xi_3} = \xi_4 \\
&\frac{d}{dt}\begin{bmatrix} \xi_2 \\ \xi_4 \end{bmatrix} = b(\xi) + A(\xi)\, u \\
&= \begin{bmatrix} L_f^2 h_1\left(\Phi^{-1}(\xi)\right) \\ L_f^2 h_2\left(\Phi^{-1}(\xi)\right) \end{bmatrix} + A(\Phi^{-1}(\xi))\, u
\end{aligned} \tag{30}$$

where the components $b(\xi)$ is described in the x coordinates as

$$\begin{aligned}
b_i(x) &= L_f^2 h_i(x) \\
&= x_2^2 \langle n_i, y_{x_1 x_1}\rangle + 2\, x_2 x_4 \langle n_i, y_{x_1 x_3}\rangle + x_4^2 \langle n_i, y_{x_3 x_3}\rangle \\
&- x_2 x_4 \cot\tfrac{x_3}{2} \langle n_i, y_{x_1}\rangle + x_2^2 \sin x_3 \langle n_i, y_{x_3}\rangle
\end{aligned} \tag{31}$$

for $i = 1, 2$. If $A(x)$ is non-singular, one can define a static feedback law

$$u = A^{-1}(x)\left(-b(x) + \nu\right) \tag{32}$$

such that (30) takes a double chain integral form

$$\begin{matrix} \dot{\xi_1} = \xi_2 \\ \dot{\xi_3} = \xi_4 \end{matrix} \quad \text{and} \quad \begin{matrix} \dot{\xi_2} = \nu_1 \\ \dot{\xi_4} = \nu_2. \end{matrix} \tag{33}$$

C. Non-singularity of The Decoupling Matrix $A(x)$

In this subsection, we analyze the non-singularity condition for the decoupling matrix (28). The matrix A has a form

$$A(x) = \begin{bmatrix} \csc^2\frac{x_3}{2} & 0 \\ 0 & 4 \end{bmatrix} \bar{A}(x) \tag{34}$$

where

$$\bar{A}(x) := \begin{bmatrix} \langle n_1, y_{x_1}\rangle & \langle n_1, y_{x_3}\rangle \\ \langle n_2, y_{x_1}\rangle & \langle n_2, y_{x_3}\rangle \end{bmatrix} \tag{35}$$

It is clear that the non-singularity of $A(x)$ depends on the non-singularity of $\bar{A}(x)$ if $x_3 \neq 0$. We suppose that

$$\operatorname{rank}\{y_{x_1}(x), y_{x_3}(x)\} = 2. \tag{36}$$

This condition is equivalent to

$$T_{y(x_1,x_3)}\mathbb{S}^2 = \operatorname{span}\{y_{x_1}, y_{x_3}\} \tag{37}$$

where $T_{y(x)}\mathbb{S}^2$ denotes the tangent plane of $\mathbb{S}^2$ at a point $y(x)$. For the given frame $\{n_1, n_2, n_3\}$, let x^* be a point which satisfies $y(x^*) = n_3 \in \mathbb{S}^2 - (0, 0, \pm 1)$. The vector $y(x)$ is expanded uniquely as

$$\begin{aligned}
y(x) &= \sum_{i=1}^{3} \langle n_i, y(x)\rangle\, n_i \\
&= a(x) n_1 + b(x) n_2 + c(x) n_3
\end{aligned} \tag{38}$$

and also its partial derivatives are expanded as

$$\begin{aligned}
y_{x_j}(x) &= \sum_{i=1}^{3} \langle n_i, y_{x_j}(x)\rangle\, n_i \\
&= a_{x_j} n_1 + b_{x_j} n_2 + c_{x_j} n_3
\end{aligned} \tag{39}$$

for $j = 1, 3$. The above decompositions are clearly obtained from projections onto the orthogonal basis. We now define

$$N := \begin{bmatrix} n_1^T \\ n_2^T \\ n_3^T \end{bmatrix} \in \mathbb{R}^{3\times 3} \tag{40}$$

and observe that $N^T N = N N^T = I \in \mathbb{R}^{3\times 3}$ and

$$\begin{aligned}
N y_{x_j} &= [\langle n_1, y_{x_j}\rangle,\, \langle n_2, y_{x_j}\rangle,\, \langle n_3, y_{x_j}\rangle]^T \\
&= [a_{x_j}, b_{x_j}, c_{x_j}]^T \in \mathbb{R}^3
\end{aligned} \tag{41}$$

We will characterize the tangent space $T_{y(x)}\mathbb{S}^2$ for fixed x by the frame $\{n_1, n_2, n_3\}$. Since $T_y\mathbb{S}^2 \subset \mathbb{R}^3$, one can construct another orthonormal base of $T_y\mathbb{S}^2$ as

$$\begin{aligned}
v_1 &= \alpha_1 n_1 + \beta_1 n_2 + \gamma_1 n_3 \\
v_2 &= \alpha_2 n_1 + \beta_2 n_2 + \gamma_2 n_3
\end{aligned} \tag{42}$$

where $\langle v_1, v_2\rangle = \alpha_1\alpha_2 + \beta_1\beta_2 + \gamma_1\gamma_2 = 0$ such that

$$\operatorname{span}\{y_{x_1}, y_{x_3}\} = \operatorname{span}\{v_1, v_2\}. \tag{43}$$

Using (39) and (43), we can decompose y_{x_j} into a linear combination of v_1 and v_2 as

$$y_{x_j} = \sum_{i=1}^{2} \langle y_{x_j}, v_i\rangle\, v_i. \tag{44}$$

We can also write

$$\begin{aligned}
\langle n_1, y_{x_j}\rangle &= \alpha_1\left(\alpha_1 a_{x_j} + \beta_1 b_{x_j} + \gamma_1 c_{x_j}\right) \\
&+ \alpha_2\left(\alpha_2 a_{x_j} + \beta_2 b_{x_j} + \gamma_2 c_{x_j}\right) \\
\langle n_2, y_{x_j}\rangle &= \beta_1\left(\alpha_1 a_{x_j} + \beta_1 b_{x_j} + \gamma_1 c_{x_j}\right) \\
&+ \beta_2\left(\alpha_2 a_{x_j} + \beta_2 b_{x_j} + \gamma_2 c_{x_j}\right)
\end{aligned} \tag{45}$$

for $j = 1, 3$. In order to simplify notations, we introduce the following matrices

$$B := \begin{bmatrix} \alpha_1 & \alpha_2 \\ \beta_1 & \beta_2 \end{bmatrix}, \tag{46}$$

$$D(x) := \begin{bmatrix} d_{11} & d_{12} \\ d_{21} & d_{22} \end{bmatrix} =$$

$$\begin{bmatrix} \alpha_1 a_{x_1} + \beta_1 b_{x_1} + \gamma_1 c_{x_1} & \alpha_1 a_{x_3} + \beta_1 b_{x_3} + \gamma_1 c_{x_3} \\ \alpha_2 a_{x_1} + \beta_2 b_{x_1} + \gamma_2 c_{x_1} & \alpha_2 a_{x_3} + \beta_2 b_{x_3} + \gamma_2 c_{x_3} \end{bmatrix}. \tag{47}$$

From above expressions we obtain,

$$\bar{A}(x) = BD(x) = \begin{bmatrix} \alpha_1 d_{11} + \alpha_2 d_{21} & \alpha_1 d_{12} + \alpha_2 d_{22} \\ \beta_1 d_{11} + \beta_2 d_{21} & \beta_1 d_{12} + \beta_2 d_{22} \end{bmatrix}. \tag{48}$$

Lemma 4.1: If the rank condition (36) holds then $D(x)$ is non-singular.

Proof: If the rank condition (36) is satisfied, it would follow that tuples of coefficients $\{a_{x_j}, b_{x_j}, c_{x_j}\}_{j=1,3}$ of y_{x_j} in (39) are linearly independent. One can find orthonormal basis in (43) with coefficients $\{\alpha_k, \beta_k, \gamma_k\}_{k=1,2}$, such that they are also linearly independent. Thus, it implies that the

rows of $D(x)$ is linearly independent. Similarly, the columns of $D(x)$ are also linearly independent. ■

Proposition 4.1: If the rank condition (36) holds then $\det \bar{A}(x) = 0$ if and only if $y(x) \in \text{span}\{n_1, n_2\}$.

Proof: First, we will show the 'if' part. Let us write $y(x) = a(x)n_1 + b(x)n_2$ with $a^2 + b^2 = 1$ and $a \neq 0$, $b \neq 0$. It would follow that,

$$y_{x_j} \in \text{span}\{n_3, n_3 \times y\} = \text{span}\{n_3, an_2 - bn_1\} \tag{49}$$

because $y_{x_j} \perp y$. Using (43) we can write, $\gamma_1 = 1, \alpha_1 = \beta_1 = 0$ and $\alpha_2 = -b, \beta_2 = a, \gamma_2 = 0$. By Lemma 4.1, D is non-singular and

$$B = \begin{bmatrix} 0 & -b \\ 0 & a \end{bmatrix}.$$

If $y \in \text{span}\{n_1\}$, $y_{x_j} \in \text{span}\{\beta_1 n_2 + \gamma_1 n_3, \beta_2 n_2 + \gamma_2 n_3\}$ for $j = 1, 3$. Thus,

$$B = \begin{bmatrix} 0 & 0 \\ \beta_1 & \beta_2 \end{bmatrix}.$$

Similarly, if $y = n_2$, $y_{x_j} \in \text{span}\{\alpha_1 n_1 + \gamma_1 n_3, \alpha_2 n_1 + \gamma_2 n_3\}$ for $j = 1, 3$ then $\beta_1 = \beta_2 = 0$ in B. Therefore, $\det \bar{A}(x) = 0$ if $y \in \text{span}\{n_1, n_2\}$. Next, we will show the 'only if' part. Since $D(x)$ is non-singular by Lemma 4.1, the non-singularity is determined by B. From (37) we conclude that $B \neq 0$. Assume that all elements of B are not zero. Then, the linear independency of v_1 and v_2 implies that $\det B \neq 0$. Hence, only possibility of $\det B = 0$ is either one of columns or rows vector is zero. In fact, a condition $\alpha_1 = \beta_1 = 0$ implies that

$$\begin{aligned} \{\text{span}\{v_1, v_2\}\}^\perp &= \{\text{span}\{\alpha_2 n_1 + \beta_2 n_2, \gamma_1 n_3\}\}^\perp \\ &= \text{span}\{n_1, n_2\} \ni y(x). \end{aligned}$$

Similarly, other possibilities follow from the discussion in the 'if' part. ■

D. Local Stability

Using Propositions 3.1 and 4.1, one can define relative degree for the output h in (22) on $\mathbb{S}^2 - (0, 0, \pm 1)$ for both, the version and vergence control problems, and input-state linearization is possible. One obtains the corresponding linear systems (33) on the ξ-coordinates. Local stabilization of the linear systems are possible by finding real coefficients such that a matrix

$$\begin{bmatrix} 0 & 1 \\ c_1 & c_2 \end{bmatrix} \tag{50}$$

is Hurwitz, i.e., real parts of all eigenvalues of the matrix are negative. In x-coordinate, the stabilizing control is given by

$$\begin{aligned} \begin{bmatrix} \nu_1 \\ \nu_2 \end{bmatrix} &= \begin{bmatrix} c_1 \xi_1 + c_2 \xi_2 \\ d_1 \xi_3 + d_2 \xi_4 \end{bmatrix} \\ &= \begin{bmatrix} c_1 h_1(x) + c_2 L_f h_1(x) \\ d_1 h_2(x) + d_2 L_f h_2(x) \end{bmatrix} \end{aligned} \tag{51}$$

for some coefficients c_i and d_i for $i = 1, 2$.

Next, we consider local stability of the target direction $y^* = \pm n_3 = y(x^*) \in \mathbb{S}^2 - (0, 0, \pm 1)$. Let $\mathcal{X}$ represent either $\mathcal{X}_{\mathbf{LIST}}$ or $\mathcal{X}_{\mathbf{MS}}$ in (15). Define a set

$$\mathcal{X}_+ := \{x = (x_1, x_3) \in \mathcal{X} \,|\, \langle n_3, y(x) \rangle > 0\}, \tag{52}$$

and in a similar manner, define $\mathcal{X}_-$ and $\mathcal{X}_0$ on which the value of the inner products is negative or zero, respectively. Since, by proposition 4.1, the relative degree does not exist on $\mathcal{X}_0$, input-state linearization is not possible on $\mathcal{X}_0 \subset \mathcal{X}$. Since y is continuous on $\mathcal{X}$ and $\{y \in \mathbb{S}^2 \,|\, \langle n_3, y \rangle \neq 0\}$ is open, $\mathcal{X}_\pm$ are open subsets of $\mathcal{X}$. Then, in the state space, there exists an open neighborhood U of $(x^*, 0)$ in $\mathcal{X} \times \mathbb{R}^2$ such that the control (32) and the stabilization control (51) renders $(x^*, 0)$ an equilibrium point and locally asymptotically stable, where the local stability result follows from [15]. Similarly, replacing $y(x^*) = n_3$ with $y(x^*) = -n_3$, we have the same conclusion. Finally, we have the following result on feedback stabilization.

Theorem 4.1: The feedback control (32) with the frame $\{n_1, n_2, n_3\}$ changes the original system into non-interacting linear subsystems (33) in ξ-coordinate. Additional feedback control (51) renders $y^*(x) = \pm n_3 \in \mathbb{S}^2 - (0, 0, \pm 1)$ locally asymptotically stable.

E. Timing Control on The Geometric Path

In this subsection, we introduce an additional timing control of (ξ_3, ξ_4)-subsystem in (33) so that a trajectory satisfies $y(x(T)) = n_3$ for $0 < T < \infty$ provided that $y(x(0)) \in \rho_{n_1}$ and $(x_2(0), x_4(0)) = 0$. We now consider a reference signal tracking problem for a linearizable system without zero dynamics [15]. Given a linear exosystem $\ddot{r}(t) = \tau(t)$, a feedback controller

$$\begin{aligned} u_2(x, t) = &-L_f^2 h_2(x) + \ddot{r}(t) + d_1 (h_2 - r) \\ &+ d_2 (L_f h_2 - \dot{r}) \end{aligned} \tag{53}$$

provides us with an error dynamics for the tracking error $e(t) := \xi_2 - r(t)$ given by

$$\ddot{e} = d_1 e + d_2 \dot{e} \tag{54}$$

where initial conditions are fixed by $r(0) = \xi_3(0)$ and $\dot{\xi}_3(0) = \dot{r}(0) = 0$. Given a time $T > 0$, we define an external input $\tau(t)$, following classical $\mathcal{L}^2$-optimization methods [16], as

$$\tau(t) = \begin{cases} -\xi_3(0) \left(\frac{36}{T^4} t^2 - \frac{48}{T^3} t + \frac{12}{T^2} \right) & t \leq T \\ 0 & t > T. \end{cases} \tag{55}$$

The response of $\ddot{r} = \tau(t)$ satisfies $r(T) = \dot{r}(T) = 0$ and $r(t) = \dot{r}(t) = 0$ for all $t \geq T$. Since $r(t)$ is bounded and there is no obstruction coming from the zero dynamics, the tracking error has an exponential rate of decay, i.e, $e(t) \leq e(0) \exp(-\gamma t)$ for some $\gamma > 0$ under a proper choice of coefficients in (54).

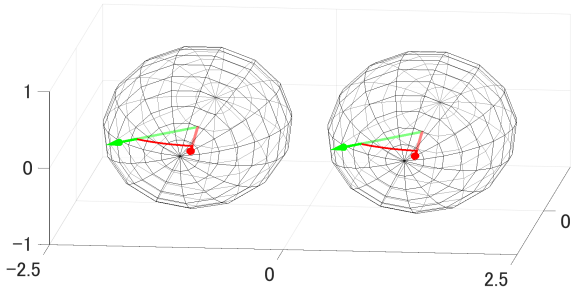

(a) Version gaze directions on $\mathbb{S}^2$. The green arrow is the initial gaze direction and the red arrow is the target direction which are the same for both the left and the right eyes.

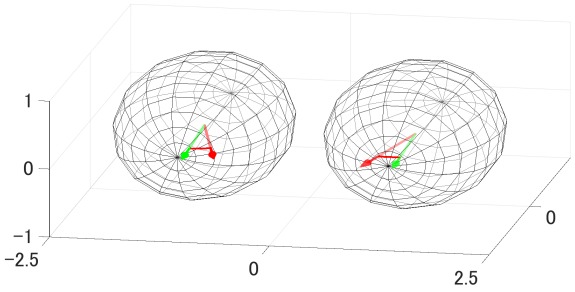

(b) Vergence gaze directions on $\mathbb{S}^2$. The color code on the arrows are same as in the version case. For the left and the right eyes, the initial gaze directions are the same, but the final target directions are different.

Fig. 3: Plots of Version and Vergence eye movements on $\mathbb{S}^2$

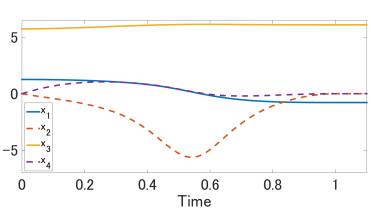

(a) States of both eyes for the version case

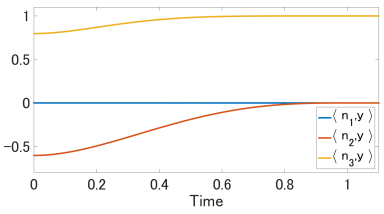

(b) Outputs h_1, h_2 and h_3 for the version case

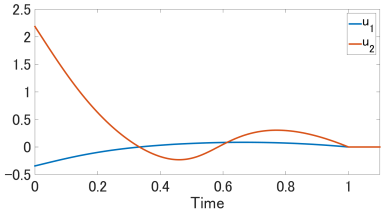

(c) Control torque inputs for the version case

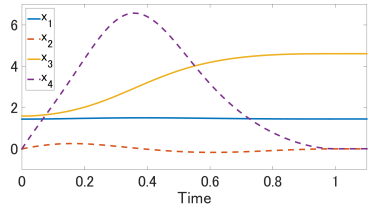

(d) States of the left eye for the vergence case

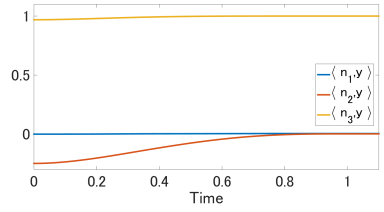

(e) Outputs from the left eye: vergence case

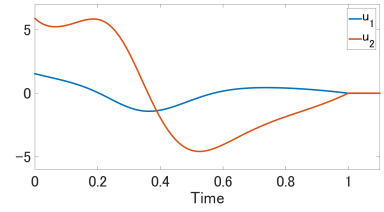

(f) Torque inputs to the left eye: vergence case

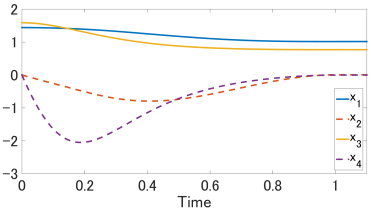

(g) States of the right eye for the vergence case

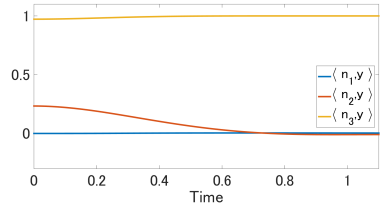

(h) Outputs from the right eye: vergence case

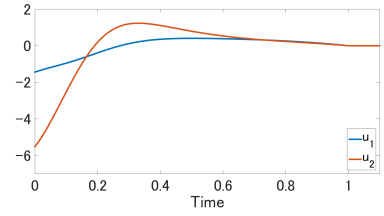

(i) Torque inputs to the right eye: vergence case

Fig. 4: States, Outputs, and Inputs from the version and vergence eye movement dynamical systems

V. SIMULATION AND DISCUSSION

In this section, we apply linearizing control law (32) to first obtain a linear system in the double chain integral form (33). Subsequently the (ξ_1, ξ_2)-subsystem is controlled with a stabilizing controller $\nu_1(x)$ from (51). The (ξ_3, ξ_4)-subsystem, on the other hand is controlled with a timing controller of the form (53). The control signals are computed for both, the version and vergence cases. The versional gaze directions are identical for the left and the right eyes. The vergence gaze directions are not identical.

We suppose that, for both version and vergence cases, the eyes start to move to a target direction at rest. Let y_{vs}, y_{vg_L}, and $y_{vg_R} \in \mathbb{S}^2 - (0, 0, \pm 1)$ be gaze directions of version case and both left and right eyes of vergence case. The upper script '*' stands for target directions. For the version case, one applies identical control law (32) to each eyes separately, and the details of the construction of the frame $\{n_1, n_2, n_3\}$ is same as shown in section IV. For the vergence case, the target directions $y^*_{vg_L} \neq y^*_{vg_R}$, and initial directions are chosen to be $y_{vg_L}(0) = y_{vg_R}(0)$. Since, $y^*_{vs}, y^*_{vg_L}$, and $y^*_{vg_R}$ are constrained to a fixed plane in $\mathbb{R}^3$, n_1 of the frame is assigned to be normal to this plane and is given by $n_1 = y^*_{vg_L} \times y^*_{vg_R}$. We now set $n_3 = y^*_{vg_L}$, for the left eye (respectively set $n_3 = y^*_{vg_R}$, for the right eye) and then write $n_2 = n_1 \times n_3$.

During simulation, all conditions are set as follows. For the version case,

$$\begin{aligned} y_{vs}(0) &= [\ 0.8554 \ \ -0.4938 \ \ 0.1564\ ]^T \in \mathbb{S}^2 \\ x_{vs}(0) &= [\ 1.2640 \ \ 0.0 \ \ 5.7386 \ \ 0.0\ ]^T \in \mathbb{R}^4 \\ y^*_{vs} &= [\ 0.9832 \ \ 0.1276 \ \ 0.1307\ ]^T \in \mathbb{S}^2. \end{aligned} \tag{56}$$

For the vergence control of the left and the right eyes we set the following.

$$\begin{aligned} y_{vg_L}(0) &= y_{vg_R}(0) = y^*_{vs} \in \mathbb{S}^2 \\ x_{vg_L}(0) &= x_{vg_R}(0) = [\ 1.4410 \ \ 0.0 \ \ 1.5878 \ \ 0.0\ ]^T \in \mathbb{R}^4 \\ y^*_{vg_L} &= [\ 0.9841 \ \ -0.1201 \ \ 0.1307\ ]^T \in \mathbb{S}^2 \\ y^*_{vg_R} &= [\ 0.9260 \ \ 0.3569 \ \ 0.1230\ ]^T \in \mathbb{S}^2. \end{aligned} \tag{57}$$

For both the version and vergence cases, the input ν_1 to stabilize (ξ_1, ξ_2)-subsystem is chosen as

$$\nu_1 = -5\, h_1(x) - 10\, L_f h_1(x). \tag{58}$$

For the timing control of (ξ_3, ξ_4)-subsystem, all parameters in (53) are set as $T = 1.0$, $d_1 = -5$, and $d_2 = -10$. The value of $\xi_3(0) = h_2(0)$ is obtained by $\langle n_2, y(0)\rangle$ where $y(0)$ is already chosen in (56) and (57).

The Figs. 3a and 3b are plots of gaze directions on S^2 for both version and vergence eye movements. Note that the versional eye movements are identical between the left and the right eye. The vergence eye movements are opposite and are required to keep the target in focus. The Figs. 4a to 4i are figures of state variables, output gaze directions, and control inputs for the version and vergence control systems. In Figs. 4b, 4e, and 4h, outputs $h_1 = \langle n_1, y\rangle$ is always zero which implies that pointing directions of all cases move along the path ρ_{n_1} in (21), and $h_2 = \langle n_2, y\rangle$ reaches zero at $t = 1$. Finally we note that $\langle n_3, y(1)\rangle = 1$ indicating that the final gaze directions coincide with n_3.

VI. CONCLUSIONS

In this paper, we have proposed a feedback controller based on Input-State linearization in order to solve version and vergence eye movement control problems. Our feedback control law renders a desirable target direction locally asymptotically stable and with additional path-following controller design, eye pointing directions move along a pre-selected path. Numerical simulation results have confirmed the effectiveness of our synthesized control law.

ACKNOWLEDGMENT

We would like to acknowledge prior work and collaboration with Indika Wijayasinghe and Methma M. Rajamuni on binocular control.

REFERENCES

[1] D. Tweed and T. Vilis, "Implications of rotational kinematics for the oculomotor system in three dimensions," *J. of Neurophysiology*, vol. 58, pp. 832–849, 1987.

[2] ——, "Geometric relations of eye position and velocity vectors during saccades," *Vision Res.*, vol. 30, pp. 111–127, 1990.

[3] A. D. Polpitiya, W. P. Dayawansa, C. F. Martin, and B. K. Ghosh., "Geometry and control of human eye movements," *IEEE Trans. on Aut. Contr*, vol. 52 (2), pp. 170–180, 2007.

[4] B. K. Ghosh, I. Wijayasinghe, and S. D. Kahagalage, "A geometric approach to head/eye control," *IEEE Access*, vol. 2, pp. 316–332, 2014. [Online]. Available: http://dx.doi.org/10.1109/ACCESS.2014.2315523

[5] I. B. Wijayasinghe, E. Aulisa, U. Büttner, B. K. Ghosh, S. Glasauer, and O. Kremmyda, "Potential and optimal control of the human head/eye complex," *IEEE Trans. on Control Systems Technology*, 2014. [Online]. Available: http://dx.doi.org/10.1109/TCST.2014.2335115

[6] L. J. V. Rijn and A. V. V. D. Berg, "Binocular eye orientation during fixations: Listings law extended to include eye vergence," *Vision Res.*, vol. 33, pp. 691–708, 1993.

[7] N. K., *Kinematics of normal and strabismic eyes*, K. Ciuffreda and C. Schor, Eds. Butterworths, 1983. [Online]. Available: http://visionlab.harvard.edu/members/ken/Papers/031butterworths83.pdf

[8] M. M. Rajamuni, E. Aulisa, and B. K. Ghosh, "Optimal control problems in binocular vision," *The 19^{th} World Congress of the International Federation of Automatic Control, Cape Town, South Africa*, pp. 5283–5289, Aug. 24-29, 2014.

[9] I. Wijayasinghe and B. K. Ghosh, "Binocular eye tracking control satisfying hering's law," *The IEEE Conference on Decision and Control, Firenze, Italy*, pp. 6475–6480, Dec. 10-13, 2013.

[10] B. K. Ghosh and I. Wijayasinghe, "Dynamics of human head and eye rotations under Donders constraint," *IEEE Trans. on Automat. Contr*, vol. 57 (10), pp. 2478–2489, 2012.

[11] I. Wijayasinghe, J. Ruths, U. Büttner, B. K. Ghosh, S. Glasauer, O. Kremmyda, and J.-S. Li, "Potential and optimal control of human headmovement using Tait-Bryan parametrization," *Automatica*, vol. 50 (2), pp. 519–529, 2014.

[12] A. J. Hanson, *Visualizing Quaternions*. Morgan Kaufmann, 2006.

[13] W. M. Boothby, *An introduction to differentiable manifolds and Riemannian geometry*. CA: Academic Press, 1986.

[14] B. K. Ghosh, T. Oki, S. D. Kahagalage, and I. Wijayasinghe, "Asymptotically stabilizing potential control for the eye movement dynamics," *Proceedings of the ASME 2014 Dynamic Systems and Control Conference, DSCC 2014, San Antonio, USA*, pp. 1–8, Oct. 22-24, 2014.

[15] A. Isidori, *Nonlinear Control Systems, 3^{rd} edition*. Springer, 1995.

[16] D. G. Luenberger, *Optimization by vector space methods*. John Wiley & Sons, 1968.

[17] H. L. Trentelman, A. A. Stoorvogel, and M. Hautus, *Control Theory for Linear Systems*. Springer, 2001.